

# Supplementary Information

## Silicon carbide coated with TiO<sub>2</sub> with enhancing cobalt active phase dispersion for Fischer–Tropsch synthesis

Yuefeng Liu,<sup>a\*</sup> Ileana Florea,<sup>b</sup> Ovidiu Ersen,<sup>b</sup> Cuong Pham–Huu <sup>a\*</sup>, Christian Meny,<sup>b</sup>

- a. Institut de Chimie et Procédés pour l’Energie, l’Environnement et la Santé (ICPEES), UMR 7515, CNRS-Université de Strasbourg (UdS), 25, rue Becquerel, 67087 Strasbourg Cedex 08, France
- b. Institut de Physique et Chimie des Matériaux de Strasbourg (IPCMS), UMR 7504, CNRS-Université de Strasbourg (UdS), 23, rue du Loess, 67034 Strasbourg Cedex 02, France

**\* To whom all correspondence should be addressed**

E-mail: yuefeng.liu@unistra.fr

cuong.pham-huu@unistra.fr

Tel. (33) 3 68 85 26 67, Fax. (33) 3 68 85 26 74

## Experimental details

### *xTiO<sub>2</sub>-SiC support preparation*

$\beta$ -SiC was synthesized via a gas–solid reaction between SiO vapor and dispersed solid carbon. The detailed synthesis of the SiC-based materials was summarized in recent reviews.<sup>1, 2</sup> The supports were prepared by pore volume impregnation of the high porosity  $\beta$ -SiC with an ethanol solution of Ti(iOC<sub>3</sub>H<sub>7</sub>)<sub>4</sub>. After impregnation, the samples were allowed to dry at room temperature for 4 h and then oven-dried at 110 °C in air for 8 h. The transformation of the titanium precursor into TiO<sub>2</sub> crystalline phase is performed by calcination of the sample in air at 600 °C for 5 h with a heating rate of 2 °C/min. The supports are noted xTiO<sub>2</sub>-SiC with x representing the loading of TiO<sub>2</sub> on the SiC carrier (5 wt. %, 10 wt. % and 15 wt. %) and marked as TS-C5, TS-C10 and TS-C15 where C means coated catalyst. The titania decorated  $\beta$ -SiC was synthesized by mixing micro-sized silicon powder and TiO<sub>2</sub> nanoparticles with a carbon-containing resin.<sup>3</sup> The mixture was further carbonized at 1300 °C under an argon atmosphere, the obtained TiO<sub>2</sub>-doped SiC material was named as TS-D where D means doped catalyst.

### *Co<sub>3</sub>O<sub>4</sub>/xTiO<sub>2</sub>-SiC catalyst preparation*

The cobalt was deposited onto the TiO<sub>2</sub> coated SiC support (TS-C10, 10 wt. % TiO<sub>2</sub>) by pore volume impregnation with cobalt nitrate (Arcros) solution. The cobalt loading was kept at 10 wt. % with respect to the support weight which is the lower range of cobalt loading according to the literature and patent survey.<sup>4, 5</sup> After impregnation the solid was allowed to dry at room temperature for 4 h and then oven-dried at 110 °C for 8 h and calcined at 350 °C (heating rate of 1 °C·min<sup>-1</sup>) for 2 h in order to obtain the Co<sub>3</sub>O<sub>4</sub>/TS-C10 catalyst precursor. The oxide form of the cobalt was further reduced in flowing hydrogen (30 mL·min<sup>-1</sup>·g<sub>cat</sub><sup>-1</sup>) at 300 °C for 6 h, to obtain the metallic ones. The obtained catalyst was noted as 10CTS-C10. The TiO<sub>2</sub> doped SiC supported cobalt catalyst and SiC-supported cobalt catalyst without TiO<sub>2</sub> were prepared following by the same process, and noted as 10CTS-D and 10CS, respectively. High loading cobalt catalyst (30 wt %) was also prepared by the same process mentioned above, and noted as 30CTS-C10.

### *Characterization techniques*

X-ray diffraction (XRD) measurements were carried out in a Bruker D-8 Advance diffractometer equipped with a Vantec detector. The powdered sample was packed onto a glass slide. ASTM powder diffraction files were used to identify the phase present in the sample. Crystallite sizes were calculated from line broadening using the Scherrer equation.

The specific surface area of the support and the catalyst, after reduction, were determined in a Micromeritics sorptometer. Before analysis the sample was outgassed at 250 °C under vacuum for 8 h in order to desorb moisture and adsorbed species on its surface. The measurements were carried out using N<sub>2</sub> as adsorbent at liquid N<sub>2</sub> temperature at relative pressures between 0.06 and 0.99.

Scanning electron microscopy (SEM) analyses were carried out on a JEOL 6700F microscope working at 10 kV accelerated voltage. The solid was fixed on the sample holder by a graphite paste for examination. Before analysis the sample was covered by a thin layer of gold in order to avoid charging effect.

TEM tomography was done on a JEOL 2100 F (FEG) electron microscope operating at a beam voltage of 200 kV, using a 2048 × 2048 pixels Ultrascan cooled CCD array detector, and a high tilt sample holder. The sample preparation for classical and tomography TEM was done according to the following process: the solid was crushed in a mortar into a very fine powder. The powder was then dispersed in ethanol by sonication during 5 min. After sonication a drop of the solution was deposited on a holey carbon copper grid and the solvent was evaporated at room temperature before introducing of the sample holder into the microscope chamber.

<sup>59</sup>Co NMR experiments were performed in a home-made zero magnetic field at a temperature of 2, 4.2 and 77K. The integrated spin-echo intensity was recorded every 0.61 MHz using a coherent pulsed NMR spectrometer with phase-sensitive detection and automated frequency scanning. The NMR spectra were taken at five different values of the excitation RF field, covering a range over more than one order of magnitude. Such a procedure allowed us to determine the optimum excitation field at each frequency and to correct for the variation of the local electronic susceptibility and thus of the NMR enhancement factor as a function of frequency. After this a further correction for the usual<sup>2</sup>

frequency dependence of the NMR signal was applied. The NMR amplitudes obtained in such a way represent the true distribution of nuclei with a given HF. Detailed description of the technique can be found in the literature.<sup>6, 7</sup> The analysis was performed on both fresh and spent catalysts; this later was covered with a homogeneous solid waxes layer, in order to prevent any surface oxidation of the cobalt phase during air exposure.

### *Fischer-Tropsch synthesis reaction*

The Fischer-Tropsch synthesis reaction was carried out in a tubular fixed-bed stainless steel reactor (*I.D.* = 6 mm) with circulating silicon oil as heating source. The reduced catalyst (5 g, in a grain form with an average size between 150 to 400  $\mu\text{m}$ ) was hosted between quartz wool plugs in the middle of the reactor. The reactor pressure was slowly increased from 0.1 to 4 MPa (ramping rate of 1 MPa·h<sup>-1</sup>) under argon. The total pressure was controlled by a back pressure regulator (MFI Ltd.). At 4 MPa the reactor temperature was raised from room temperature to the desired reaction temperature (heating rate of 2°C·min<sup>-1</sup>). Then, the argon flow was replaced by a 50:50 v:v mixture of synthesis gas and argon (CO:H<sub>2</sub> = 1:2). The catalyst was activated under a synthesis gas-argon mixture with different synthesis gas concentrations during three days before evaluation under pure synthesis gas conditions. The catalyst bed temperature was monitored with a thermocouple ( $\varnothing$  0.3 mm) inserted inside a stainless steel finger ( $\varnothing$  1 mm) passing through the catalyst bed. The products were condensed in two high pressure traps maintained at 85°C and 15°C respectively. The exit gas was analyzed on-line, both by Thermal Conductivity Detector (TCD) and Flame Ionization Detector (FID), with a gas chromatography (GC Varian 3800 equipped with a DP-1 and Carbobond capillary columns).

The liquid hydrocarbon phase and water were condensed in the traps and were analyzed off-line at the end of the test. The water was removed from the organic phase by decantation of the system. A known amount (100 mg) of the organic phase, liquid hydrocarbons and waxy products, was dissolved in 3 mL of dichloromethane under sonication during 30 minutes. Then, 20 mL of CS<sub>2</sub> were further added to the solution in order to ensure the complete dissolution of the organic phase. For analysis, 1  $\mu\text{L}$  of the solution was injected in a GC apparatus equipped with a Simdist column operated at 400 °C which allowed the detection of hydrocarbons from C<sub>9</sub> to C<sub>70</sub>.

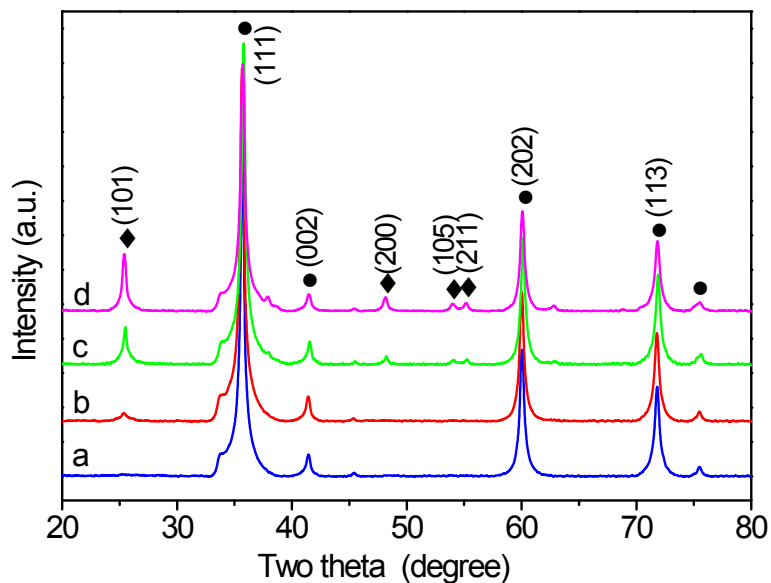


**Figure S1.** X-ray diffraction patterns of various  $\text{TiO}_2$  loading on high porosity SiC: (a) SiC; (b) TS-C5; (c) TS-C10, (d) TS-C15. Diamond ( $\blacklozenge$ ): anatase  $\text{TiO}_2$ ; circles ( $\bullet$ ): SiC.

The crystal structure and composition of the different supports are characterized by wide-angle XRD. As can be seen in Figure S1, XRD patterns of the  $x\text{TiO}_2\text{-SiC}$  show four resolved diffraction peaks, located at  $25^\circ$ ,  $48^\circ$ ,  $55^\circ$  and  $56^\circ$ , which can be assigned to the (101), (200), (105) and (211) reflections of the anatase  $\text{TiO}_2$  phase.<sup>8, 9</sup> The results indicate that the obtained  $\text{TiO}_2$  layer is well crystallized in single anatase phase. The diffraction lines of the anatase  $\text{TiO}_2$  phase become more intense as a function of the deposited  $\text{TiO}_2$ . The crystal size determined by the Scherrer formula is about 25, 39 and 40 nm for  $\text{TiO}_2$  loading going from 5 wt % to 15 wt %, respectively. The diffraction peaks of SiC found in the XRD patterns confirm the presence of face-centered-cubic ( $\beta$ -SiC) with the stacking faults of hexagonal ( $\alpha$ -SiC). The diffraction peak of  $\alpha$ -SiC at  $2\theta = 33.7^\circ$  is appeared as the stacking faults along the growth direction (111) of  $\beta$ -SiC, and according to the HR-TEM study of the SiC published previously.<sup>1, 10</sup>

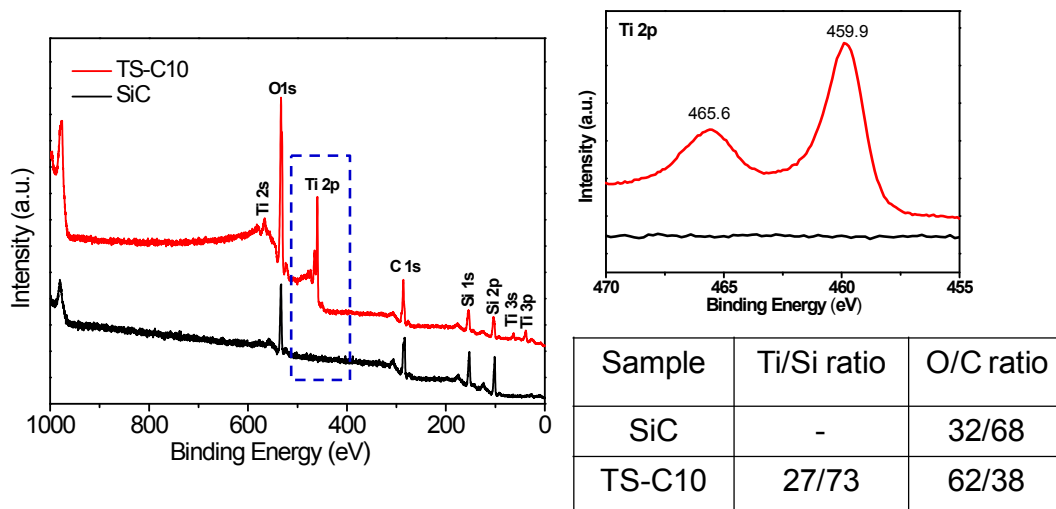


**Figure S2.** Survey XPS spectra and high-resolution Ti2p XPS spectra of SiC and TS-C10 samples

X-ray photoelectron spectroscopy (XPS) measurements were carried out to examine the valence states of Ti element in  $\text{TiO}_2$  coated SiC. As shown in Figure S2, the survey scan spectrum confirms the existence of Ti, O, C and Si elements. Figure S2 also presents the XPS spectra of Ti 2p doublet peaks; the binding energy of Ti  $2p_{1/2}$  and Ti  $2p_{3/2}$  was observed at approximately 465.6 eV and 459.9 eV, respectively. The splitting data between the Ti  $2p_{1/2}$  and Ti  $2p_{3/2}$  core levels are 5.7 eV, indicating a normal state of  $\text{Ti}^{4+}$  in the anatase  $\text{TiO}_2$ .

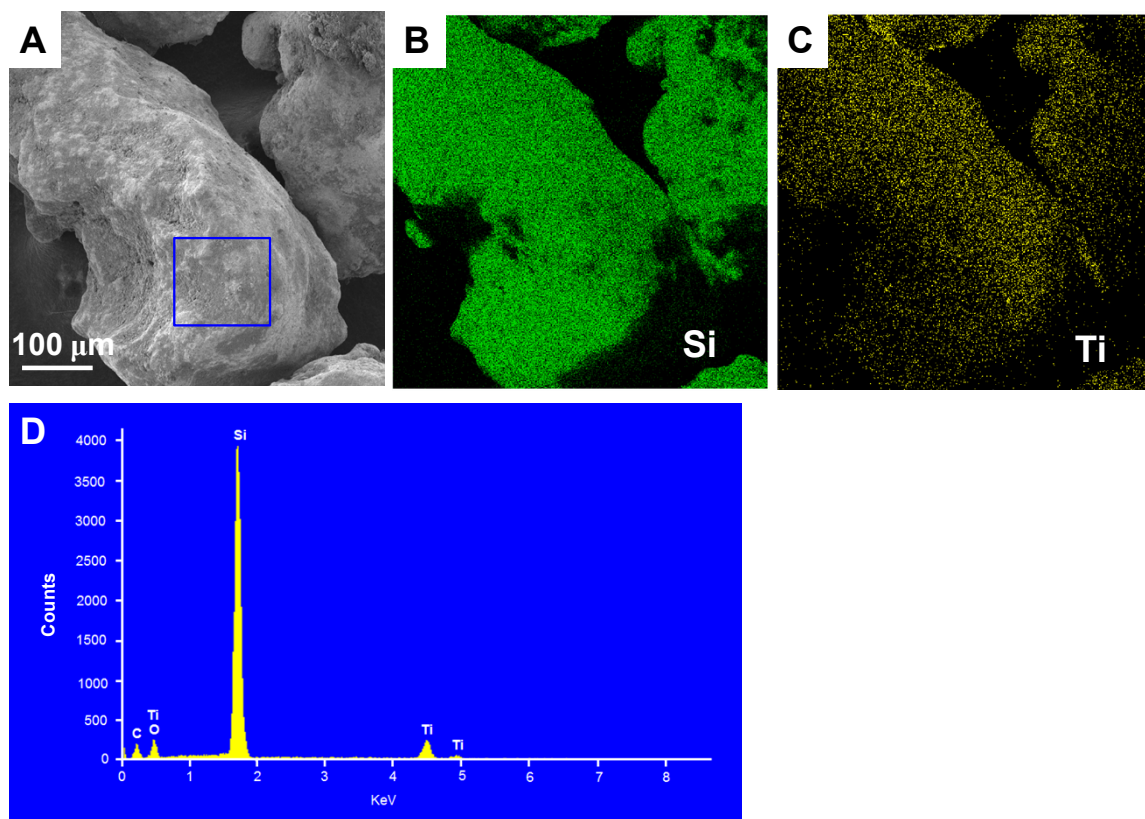


**Figure S3.** SEM-EDX micrographs of granular TS-C10 support. (A) SEM image of the SiC particle coated with TiO<sub>2</sub>; (B, C) Silicon and titanium EDX maps of the same particle surface shown in (A); (D) EDX in the square area from the image in (A).

The elemental composition of the TiO<sub>2</sub> coated SiC sample is investigated by EDX and the corresponding mapping images (TS-C10), are presented in Figure S3. SEM image and EDX mapping reveal the similar trends of morphologies and elemental distribution (see Si map and Ti map), and confirm the homogeneous coating of the support (Figure S3 C). The EDX analysis from the marked square area in Figure S3 A is presented in Figure S3 D.

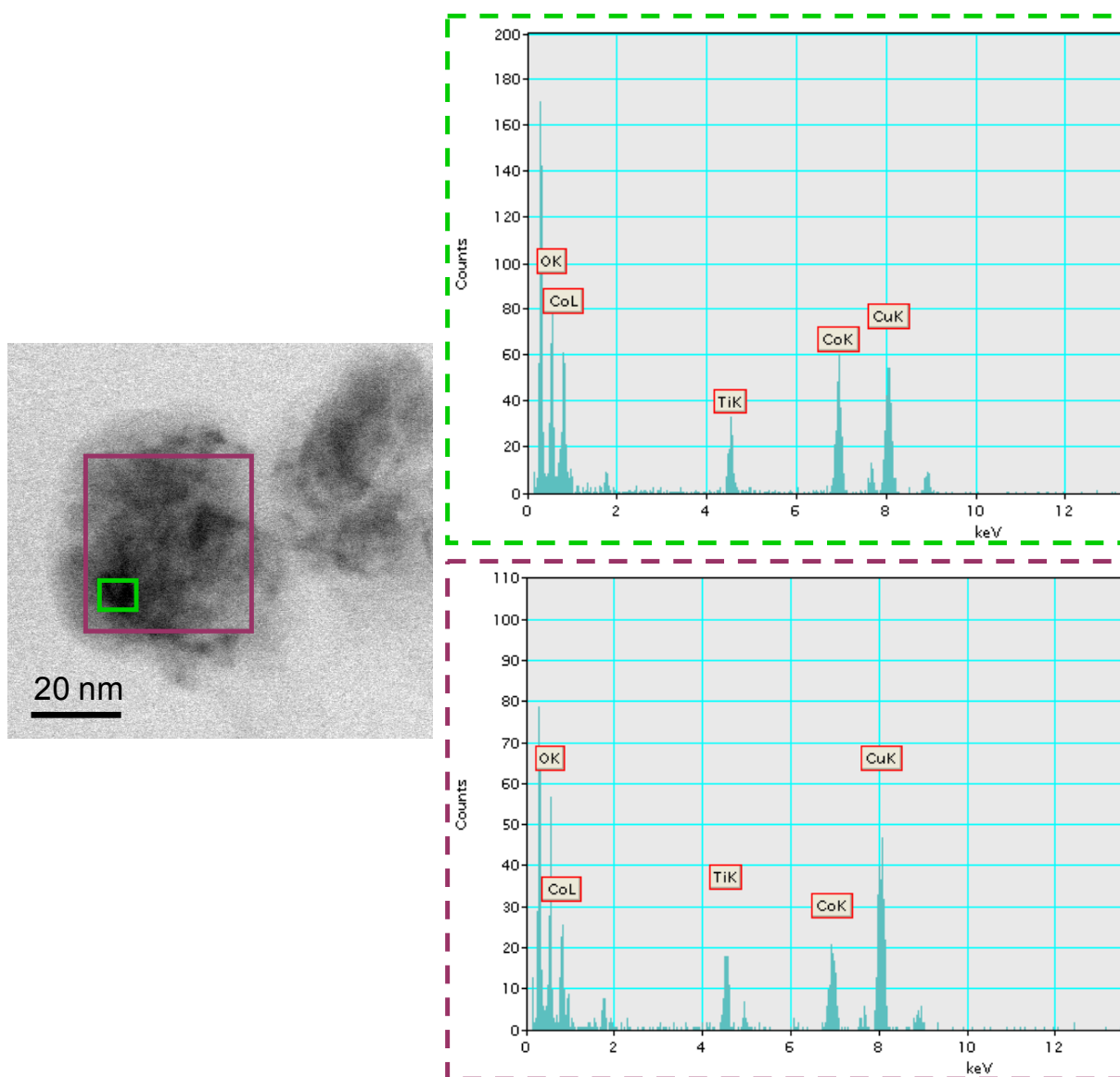


**Figure S4.** Typical TEM image and energy-dispersive X-ray spectroscopy (EDX) of 10CTS-C10 sample.



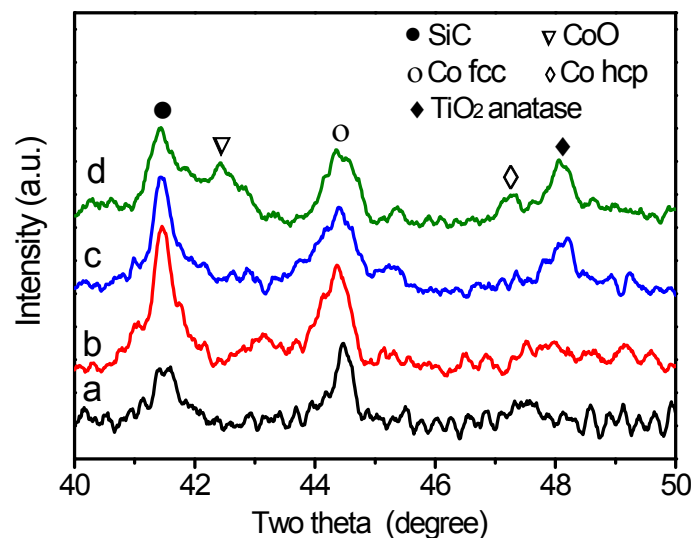


**Figure S5.** Ex situ X-ray diffraction patterns of prepared catalysts: (a) 10CS ; (b) 10CTS-C5; (c) 10CTS-C10 and (d) 10CTS-C15

The XRD patterns of the cobalt supported on the SiC-based catalysts are presented in Figure S5. Before XRD experiments, the catalysts were reduced under hydrogen at 300 °C for 6 h. The 10Co/SiC catalyst only displays diffraction lines corresponding to the SiC support and metallic cobalt phase. The absence of diffraction lines corresponding to the cobalt oxide phases confirms the complete reduction of the cobalt phase. A similar reduction pattern is also observed on the TiO<sub>2</sub> coated catalysts. However, a diffraction line appears at around 42.5° on the catalyst with 15 wt. % of TiO<sub>2</sub>, which could be assigned to a CoO phase. Such results seem to indicate that at high TiO<sub>2</sub> loading some hardly reducible phase of cobalt was formed after reduction of the catalyst.

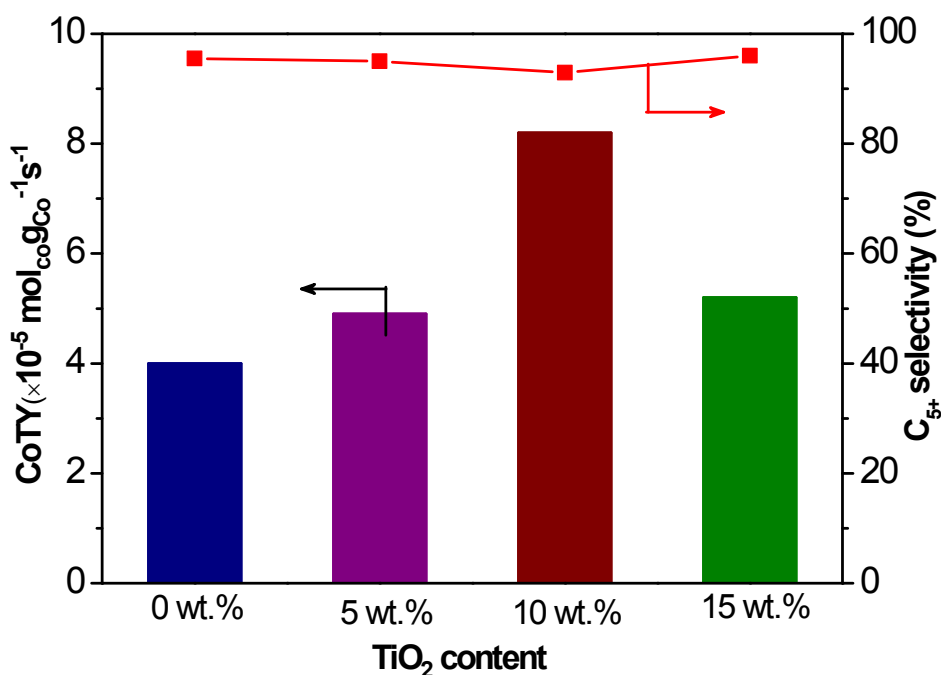


**Figure S6.** FTS activity and C<sub>5+</sub> selectivity as functions of time on stream on various TiO<sub>2</sub> loading on catalysts. Reaction conditions: H<sub>2</sub>/CO molar ratio = 2, reaction temperature = 215 °C, total pressure = 40 bar, GHSV (STP) = 60 ml·g<sub>cat</sub><sup>-1</sup>·min<sup>-1</sup>.

The CO conversion, cobalt time yield (CoTY,  $\times 10^{-5} \text{ mol}_{\text{Co}} \text{ g}_{\text{Co}}^{-1} \text{ s}^{-1}$ ) and C<sub>5+</sub> selectivity obtained on cobalt supported on TiO<sub>2</sub> coated SiC with different titania content, i.e. 5% (10CTS-C5), 10% (10CTS-C10) and 15% (10CTS-C15), are shown in Figure S6. The same cobalt catalyst supported on SiC without TiO<sub>2</sub>, noted Co/SiC, is also plotted in the same figure to compare the catalytic performance obtained under the same reaction conditions. The introduction of TiO<sub>2</sub> in the support leads to a considerable improvement of the catalyst activity for the reaction of FTS. The cobalt time yield increases from 4.0 to 4.9 mol<sub>Co</sub>g<sub>Co</sub><sup>-1</sup>s<sup>-1</sup> over the 10CTS-C5 catalyst promoted with 5 wt% TiO<sub>2</sub> comparing to TiO<sub>2</sub>-free catalyst. The CoTY of 8.2 mol<sub>Co</sub>g<sub>Co</sub><sup>-1</sup>s<sup>-1</sup> is obtained on the 10CTS-C10 at 215 °C. When the TiO<sub>2</sub> loading increases up to 15%, the cobalt time yield decreases to 5.2 mol<sub>Co</sub>g<sub>Co</sub><sup>-1</sup>s<sup>-1</sup>. This decay of the FTS activity as increasing the TiO<sub>2</sub> loading could be attributed to an increase of the metal-support interaction between the TiO<sub>2</sub> and the cobalt precursor which contributes to lower cobalt dispersion. The increase of the FTS catalytic activity is accompanied by a slight decrease of selectivity for liquid hydrocarbons. The C<sub>5+</sub> selectivity decreases from 95% for an unpromoted catalyst to about 92% for the promoted catalyst loaded with 10% of TiO<sub>2</sub>.

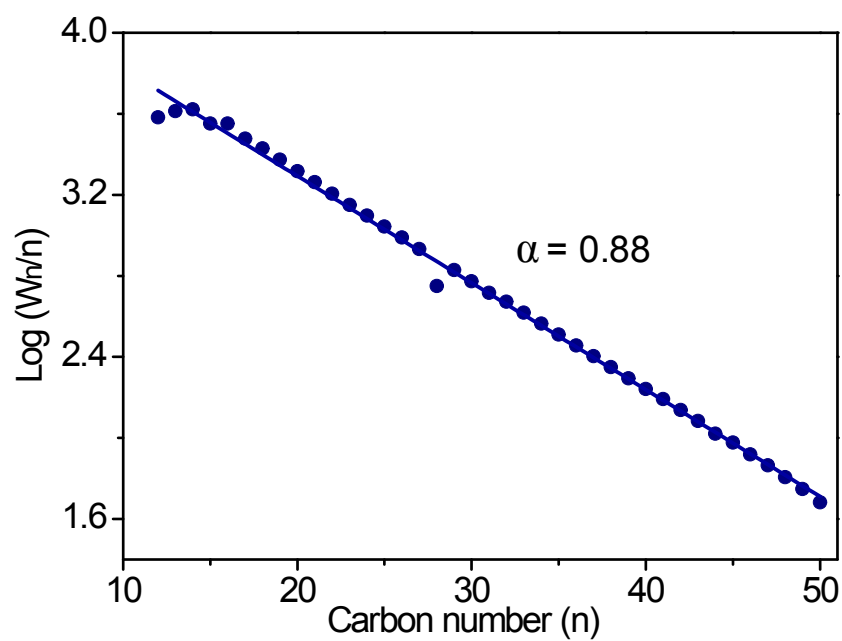


**Figure S7.** Anderson-Schulz-Flory plots for 30CTS-C10 catalyst on realistic FTS reaction conditions. Reaction conditions:  $\text{H}_2/\text{CO}$  molar ratio = 2, reaction temperature = 240 °C, total pressure = 40 bar, GHSV (STP) =  $320 \text{ mL} \cdot \text{g}_{\text{cat}}^{-1} \cdot \text{min}^{-1}$ , total pressure = 40 bar, 1.25 g catalyst diluted with 3.75g SiC.

**Table S1.** BET surface area and pore volume of the different SiC carriers and the reduced catalysts.

Sample	Surface area (m <sup>2</sup> /g)	Total pore volume (cm <sup>3</sup> /g)	BJH pore diameter (nm)
SiC	40.4	0.120	12.8
TS-C5	38.5	0.099	10.4
TS-C10	41.4	0.134	13.6
TS-C15	40.5	0.102	10.1

**Table S2** Catalytic performance on the TiO<sub>2</sub>-SiC supported 30 wt % cobalt based catalyst (30CTS-C10) at severe FTS reaction.<sup>a</sup>

CO Conv. (%)	Product selectivity (%)				r <sub>C<sub>5+</sub></sub> <sup>b</sup>	α <sup>c</sup>
	CO <sub>2</sub>	CH <sub>4</sub>	C <sub>2</sub> -C <sub>4</sub>	C <sub>5+</sub>		
35.5	0.1	9.8	4.3	85.8	1.22	0.88

<sup>a</sup> All data were obtained after 20h time on stream with stable catalytic performance at testing conditions. Reaction condition: T = 240 °C, 320 ml·g<sub>cat</sub><sup>-1</sup>·min<sup>-1</sup>, total pressure = 40 bar, 1.25 g catalyst diluted with 3.75g SiC.

<sup>b</sup> FTS rate to C<sub>5+</sub> hydrocarbons (g<sub>C<sub>5+</sub></sub>·g<sub>cat</sub><sup>-1</sup>·h<sup>-1</sup>, mass of C<sub>5+</sub> formed per gram catalyst per hour).

<sup>c</sup> Chain growth probability factor.

## Reference

1. P. Nguyen and C. Pham, *Appl Catal a-Gen*, 2011, **391**, 443-454.
2. Y. F. Liu, O. Ersen, C. Meny, F. Luck and P. H. Cuong, *Chemsuschem*, 2014, **7**, 1218-1239.
3. Y. Liu, B. de Tymowski, F. Vigneron, I. Florea, O. Ersen, C. Meny, P. Nguyen, C. Pham, F. Luck and C. Pham-Huu, *ACS Catalysis*, 2013, **3**, 393-404.
4. R. Oukaci, A. H. Singleton and J. G. Goodwin, *Appl Catal a-Gen*, 1999, **186**, 129-144.
5. F. Diehl and A. Y. Khodakov, *Oil Gas Sci Technol*, 2009, **64**, 11-24.
6. C. Meny and P. Panissod, ed. G. A. Webb, Springer, Heidelberg, Germany 2006.
7. P. Panissod and C. Meny, *Appl Magn Reson*, 2000, **19**, 447-460.
8. B. Jongsomjit, T. Wongsalee and P. Praserttham, *Mater Chem Phys*, 2006, **97**, 343-350.
9. J. Y. Shen, H. Wang, Y. Zhou, N. Q. Ye, G. B. Li and L. J. Wang, *Rsc Adv*, 2012, **2**, 9173-9178.
10. N. Keller, C. Pham-Huu, M. J. Ledoux, C. Estournes and G. Ehret, *Appl Catal a-Gen*, 1999, **187**, 255-268.